Contribution from the Department of Chemistry and The James Franck Institute, The University of Chicago, Chicago, Illinois 60637

A Theoretical Study of the Adsorbate-Induced Reconstruction of the (110) Surface of Nickel and a Molecular Analogue

Jeremy K. Burdett,* Paul T. Czech, and Thomas F. Fässler

Received April 15, 1991

Recent experimental data have shown that the (110) surface of nickel with adsorbed oxygen reconstructs to give a missing-row structure, but with adsorbed hydrogen, a Peierls-like pairing of these rows is found. With CO, the surface does not reconstruct at all. We show that although the row/row pair potential, calculated via the tight-binding method, is negative for the clean nickel surface, it becomes positive, indicating repulsion between the metal atoms, on adsorption of oxygen in accord with experiment. The crossing point in the potential moves toward the left of the transition-metal series on adsorption of oxygen, the extent of the movement being controlled by the size of the metal–oxygen interaction. A similar effect is calculated to occur on Ni(100). Similar results are predicted for CO on nickel, a result not in accord with experiment, but the pair potential is significantly reduced if the CO groups are arranged in the zigzag manner found experimentally. For hydrogen on nickel, it is shown how the pairing distortion is also sensitive to adsorption, being energetically favorable for hydrogen coverages greater than 1. In order to tie these results together, a simple molecular analogue is presented.

Introduction

The chemistry of surfaces is a rich and varied field. It is an area which has seen a substantial increase in our level of understanding in recent years, driven by dramatic advances in the physical methods used to study surfaces,[1-3] both clean surfaces and those where adsorbed species are present. There are several striking features concerning the atomic structure at the surface. In particular, it is clear that some surfaces reconstruct to generate surface geometries which have little resemblance to their bulk structure and that some such reconstructions are driven by the adsorption process itself. The types of reconstruction associated with surfaces of solids composed of main-group elements are relatively easy to understand, given traditional rules of chemical bonding, although it is usually not trivial to readily distinguish energetically between all types of possibilities. For example, generation of a (111) silicon surface from the solid leads to a single unshared valency at each surface atom—a dangling bond. Chemical stability may be restored by adsorption of hydrogen atoms. This leads to saturation of the severed bonds without any change in the surface topology and thus to no reconstruction. Without addition of hydrogen, the surface has to distort (or reconstruct) considerably to satisfy the free surface valencies. For transition metals the process is more complex. The description of the "dangling bonds" at a transition-metal surface, unreconstructed or not, is not a simple matter. Even when the geometrical distortion has been established experimentally, it is usually not obvious how to describe it in terms of the localized two-electron bond of main-group chemistry, even if such a model were appropriate. Adsorption of small molecules on surfaces has been studied theoretically in recent years using the same methods used to study both small molecules and solids, and a chemical picture is beginning to emerge.[4]

Although, as we have noted above, considerable advances have been made in terms of the experimental determination of these surface structures, it is certainly true to say that the quantitative details are not as well-defined experimentally as are bond lengths in small molecules or crystalline solids. So, whereas there are several types of well-ordered reconstructions on the (110) surfaces of fcc metals known, not all of the results appear equally definitive. Some of these surfaces are stable in the clean state, and some reconstruct in the presence of adsorbed atoms. Whereas the bare (110) surfaces of Ni, Cu, Rh, Pd, and Ag are stable[5] (although of course, there are small changes in metal–metal distances between the surface and the bulk), the analogous surfaces of Ir, Pt, and Au are found to transform into a (2×1) pattern, which is generally accepted to be a missing-row type of reconstruction.[5] An unreconstructed surface is observed for Ir in the presence of disordered oxygen,[5] whereas a (2×1) phase of Pd(110) is found in the presence of Cs and Na.[5] The missing-row type of reconstruction (Figure 1a) was recently established for the system (2×1)O–Ni(110)[6] after a long discussion concerning the sawtooth[7-9] model also. For the oxygen-induced (2×1) phase on Cu(110) and Ag(110) the same reconstruction models[10-12] as well as buckling-row models[13] are proposed, but no general concensus is yet found in the literature. A common feature of the three oxygen-induced (2×1) phases of the surfaces of Ni, Cu, and Ag is that oxygen is bound in all cases in the long-bridge sites.[8,10,14] This is in contrast to the case of O–Ir(110), where oxygen atoms are found in the short-bridge sites of the 110 surface.[5] Interestingly, no reconstruction occurs here. A missing-row structure which appears to be driven by the adsorbate has been reported for the adsorption of oxygen atoms on Cu(100),[15] where there is

(1) *Determination of Surface Structure by LEED*; Marcus, P. M., Jona, F., Eds.; Plenum Press: New York, 1984.
(2) Engel, T.; Reider, K. H. In *Structural Studies of Surfaces*; Hohler, G., Ed.; Vol. 91 of Springer Tracts in Modern Physics; Springer: Berlin, 1982.
(3) Ibach, H.; Mills, D. L. *Electron Energy Loss spectroscopy and Surface Vibrations*; Academic Press: New York, 1982.
(4) See the following, for example. O_2 on Ag(111): Zonnevylle, M. C.; van den Hoeck, P. J.; van Santen, R. A.; Hoffmann, R. *Surf. Sci.* **1989**, *223*, 233. Oxygen and ethylene on Ag(110): Jørgensen, K. A.; Hoffmann, R. *J. Phys. Chem.* **1990**, *94*, 3046. Hoffmann, R. *Solids and Surfaces: a Chemist's View of Bonding in Extended Structures*; Verlag Chemie: New York, 1988.
(5) For a collection of structures see: MacLaren, J. M.; Pendry, J. B.; Rous, P. J.; Saldin, D. K.; Somorjai, G. A.; Van Hove, M. A.; Vvedensky, D. D. *Surface Crystallographic Information Service, A Handbook of Surface Structures*; D. Reidel Publishing Co.: Dordrecht, The Netherlands, 1988.
(6) Kleinle, G.; Winterlein, J.; Ertl, G.; Behm, R. J.; Jona, F.; Moritz, W. *Surf. Sci.* **1990**, *225*, 171. Voigtländer, B.; Lehwald, S.; Ibach, H. *Surf. Sci.* **1990**, *225*, 162.
(7) For a review, see: Brundle, C.; Broughton, J. In *The Chemical Physics of Solid Surfaces and Heterogeneous Catalysis*; King, D. A., Woodruff, D. P., Eds.; Elsevier: New York, 1985.
(8) Schuster, M.; Varelas, C. *Surf. Sci.* **1983**, *134*, 195. Baro, A.; Binning, G.; Rohrer, H.; Gerber, Ch.; Stoll, E.; Baratoff, A.; Salvan, F. *Phys. Rev. Lett.* **1984**, *52*, 1304. Baberschke, K.; Döbler, U.; Wenzel, L.; Arvanitis, D.; Baratoff, A.; Rieder, K. *Phys. Rev. B* **1986**, *33*, 5910.
(9) Stroscio, J.; Perrson; Ho, W. *Phys. Rev. B* **1986**, *33*, 6758.
(10) Van de Riet, E.; Smeets, J.; Fluit, J.; Niehaus, A. *Surf. Sci.* **1989**, *214*, 111. Bader, M.; Puschmann, A.; Ocal, C.; Haase, J. *Phys. Rev.* **1986**, *57*, 3273.
(11) Yarmoff, J.; Cyr, D.; Huang, J.; Kim, S.; Williams, R. *Phys. Rev. B.* **1986**, *33*, 3856. Döbler, U.; Baberschke, K.; Vvedensky, D.; Pendry, J. B. *Surf. Sci.* **1986**, *178*, 679.
(12) Yang, L.; Rahman, T.; Bracco, G.; Tatarek, R. *Phys. Rev. B* **1989**, *40*, 12271.
(13) Feidenhanse'l; Stensgaard, R. *Surf. Sci.* **1983**, *133*, 453. Didio, R.; Zehner, D.; Plummer, E. *J. Vac. Sci. Technol.* **1984**, *A2*, 852. Chua, F.; Kuk, Y.; Siverman, P. *Phys. Rev. Lett.* **1989**, *63*, 386.
(14) Engel, T.; Rieder, K. *Surf. Sci.* **1984**, *148*, 321. O'Conner, D. *Surf. Sci.* **1986**, *173*, 593. Robinson, A.; Somers, J.; Richen, D.; Bradshaw, A.; Killogne, A.; Woodruff, D. *Surf. Sci.* **1990**, *227*, 237. Heiland, W.; Iberl, F.; Taglauer, E.; Menzel, D. *Surf. Sci.* **1975**, *53*, 383. Puschmann, A.; Haase, J. *Surf. Sci.* **1984**, *144*, 559. Niehus, H.; Comsa, G. *Surf. Sci.* **1985**, *151*, L171.

0020-1669/92/1331-0129$03.00/0

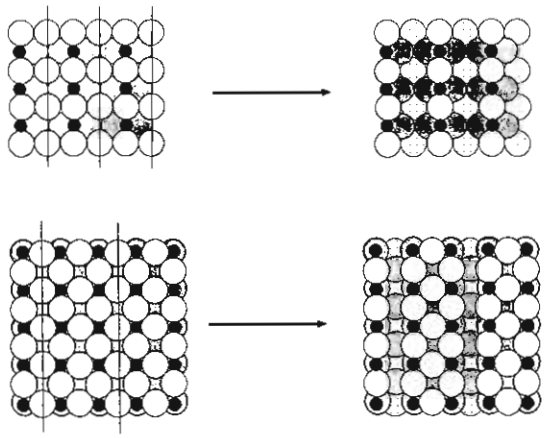

Figure 1. Missing-row reconstruction of the nickel surface as a result of oxygen adsorption: (a, top) (110) surface; (b, bottom) (100) surface. Oxygen atoms are shown as small filled circles, surface metal atoms as large open circles, second-layer metal atoms as large shaded circles, and third-layer metal atoms as large speckled circles.

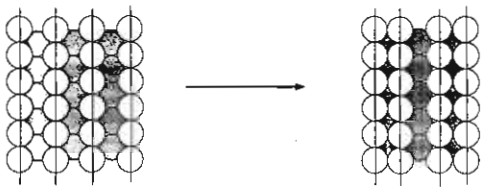

Figure 2. Pairing distortion of the surface metal atoms of Ni(110) on adsorption of hydrogen. Surface metal atoms are shown as large open circles and second layer metal atoms as large shaded circles.

a $(2\sqrt{2} \times \sqrt{2})R45°$–O pattern (Figure 1b).

A different type of adsorbate-induced reconstruction is also found in the case of hydrogen as adsorbate.[16-18] Here a hydrogen coverage of $\theta_H > 1.0$ induces a row pairing for H/Ni(110) and H/Pd(110), shown in Figure 2. A different model appears to be appropriate for H/Cu(110), such as a subsurface row pairing.[15] No reconstruction however is found with $\theta_H \leq 1.0$ for H/Ni(110), H/Rh(110),[17] and H/Pd(110). The H/Rh(110) surface does not reconstruct even if $\theta_H > 1.0$.[13]

An interesting feature is that all oxygen-induced reconstructions occur at a oxygen coverage $\theta_O = 0.5$, whereas hydrogen-induced reconstructions occur for $\theta_H > 1.0$. Here, although the location of the adsorbed hydrogen atoms is not well-defined, there is no doubt that the surface metal atoms pair as shown in a manner reminiscent of structural changes in molecules and solids described as Jahn–Teller and Peierls distortions, respectively. One of the questions we shall want to answer is whether this distortion should be regarded as a surface Peierls distortion.

Carbon monoxide appears[19] to form a (2×1) structure on the nickel (110) surface, although here is not clear whether the CO is adsorbed on a bridge or on-top sites. The arrangement of the adsorbed CO's seems quite distorted, the CO vector tilted by about 21° away from the surface perpendicular.[20] The experimental results suggest that the metal surface itself has not reconstructed. Thus, the three adsorbates, H, O, and CO, induce very different structural changes in the metal surface. We note here that they represent three distinctly different electronic problems. Hydrogen only possesses orbitals for σ interactions, oxygen is a π donor in addition, and CO is a π acceptor.

Several different theoretical approaches have been used to study problems of surface reconstruction. The embedded atom method has been used to study[21] the reconstruction of Au(100), for example. Tight-binding calculations were used[22] 10 years ago for the (100) surface of Mo and W. Since then, there have been several studies, one in particular[23] on the reconstruction of the (110) surface of Ir, Pt, and Au. In this paper, we shall address this reconstruction problem by using electronic ideas supported by tight-binding calculations within the extended Hückel formalism on metal slabs several atoms thick. The details are given in the Appendix. **1** shows the occurrence of (110) surface re-

plain surface	$\theta_O = 0.5$	$\theta_H \geq 1.0$
Ni Cu	**Ni Cu**	**Ni Cu**
Rh Pd Ag	**Ag**	**Rh Pd**
Ir Pt Au	**Ir**	

M = no reconstruction, **M** = reconstruction of the (110) surface.

1

construction for the later transition elements. It is clear that, whatever the explanation, it cannot be one which simply depends on electron count, since the same behavior is not found for all members of a group. This is in contrast to many theoretical explanations of structural problems in both main-group and transition metal-chemistry, often strongly controlled by electron count. We will present a model, extracted from the results of these computations, which will allow insight into some of these structural changes.

Electronic Structure of the Surface

We first describe some of the electronic features of the cubic close-packed (110) surface and how it changes on oxygen adsorption. Figure 3a shows the electronic density of states calculated for a nickel slab eight atoms thick whose parallel top and bottom faces are (110) surfaces. It is important to note that the Fermi level for nickel lies close to the top of the d band. Notice that the decomposition into surface and bulk densities shows a narrower band for the surface states than for the bulk, understandable in terms of the different coordination numbers. The surface band however, broadens, at the higher end especially, on addition of oxygen (Figure 3b), leading overall to surface → bulk electron transfer for the electron count appropriate for nickel. Parts c and d of Figure 3 show similar densities of states for the missing-row structure found experimentally[6] for oxygen on Ni(110) calculated for a nickel slab nine atoms thick. The differences between the two pairs, Figure 3a,b and Figure 3c,d, are rather small and do not give an obvious hint as to the origin of the reconstruction. Figure 4 shows COOP curves[24] between the metal atoms along the short axis of the unreconstructed surface with and without adsorbed oxygen. Notice that at an electron count somewhat larger than that for nickel the overlap populations go to zero. Although the COOP curve is close to zero for the nickel electron count, and becomes slightly antibonding at this point on addition of oxygen, the bond overlap population for the bare surface is 0.14 (i.e., bonding) and remains unchanged after addition of oxygen. The bond overlap population between a surface atom and an atom from the penultimate layer is a little smaller for the bare surface (0.11) and drops by a small amount (to 0.10) on coordination of oxygen. From the point of view of the density of states and the bond overlap populations, there appears to be nothing indicative of the loss of a row of metal atoms here, induced by the addition of oxygen. We need to search for another way to study this problem.

(15) Zeng, H. C.; McFarlane, R. A.; Mitchell, K. A. R. *Surf. Sci.* **1989**, *208*, L7. Zeng, H. C.; McFarlane, R. A.; Sodhi, R.; Mitchell, K. A. R. *Can. J. Chem.* **1988**, *66*, 2054.
(16) For a review see: Christmann, K. *Surf. Sci. Rep.* **1988**, *9*, 1.
(17) Voigtländer, B.; Lehwald, S.; Ibach, H. *Surf. Sci.* **1989**, *208*, 113.
(18) Kleinle, G.; Penka, V.; Behm, R. J.; Ertl, G.; Moritz, W. *Phys. Rev. Lett.* **1987**, *58*, 148.
(19) Riedel, W.; Menzel, D. *Surf. Sci.* **1985**, *163*, 39. Kuhlenbeck, H.; Neumann, M.; Freund, H.-J. *Surf. Sci.* **1986**, *173*, 194. Hannamann, D.; Passler, M. *Surf. Sci.* **1988**, *203*, 449. Voigtländer, B.; Bruckmann, D.; Lehwald, S.; Ibach, H. *Surf. Sci.* **1990**, *225*, 151.
(20) Wesner, D. A.; Coenen, F. P.; Bonzel, H. P. *Phys. Rev. Lett.* **1988**, *60*, 1045.
(21) Dodson, B. W. *Phys. Rev. B* **1987**, *35*, 880.
(22) Terakura, I.; Terakura, K.; Hamada, N. *Surf. Sci.* **1981**, *103*, 103; **1981**, *111*, 479.
(23) Brocksh, H.-J.; Bennemann, K. H. *Surf. Sci.* **1985**, *161*, 321.
(24) Hughbanks, T.; Hoffmann, R. *J. Am. Chem. Soc.* **1983**, *105*, 3528.

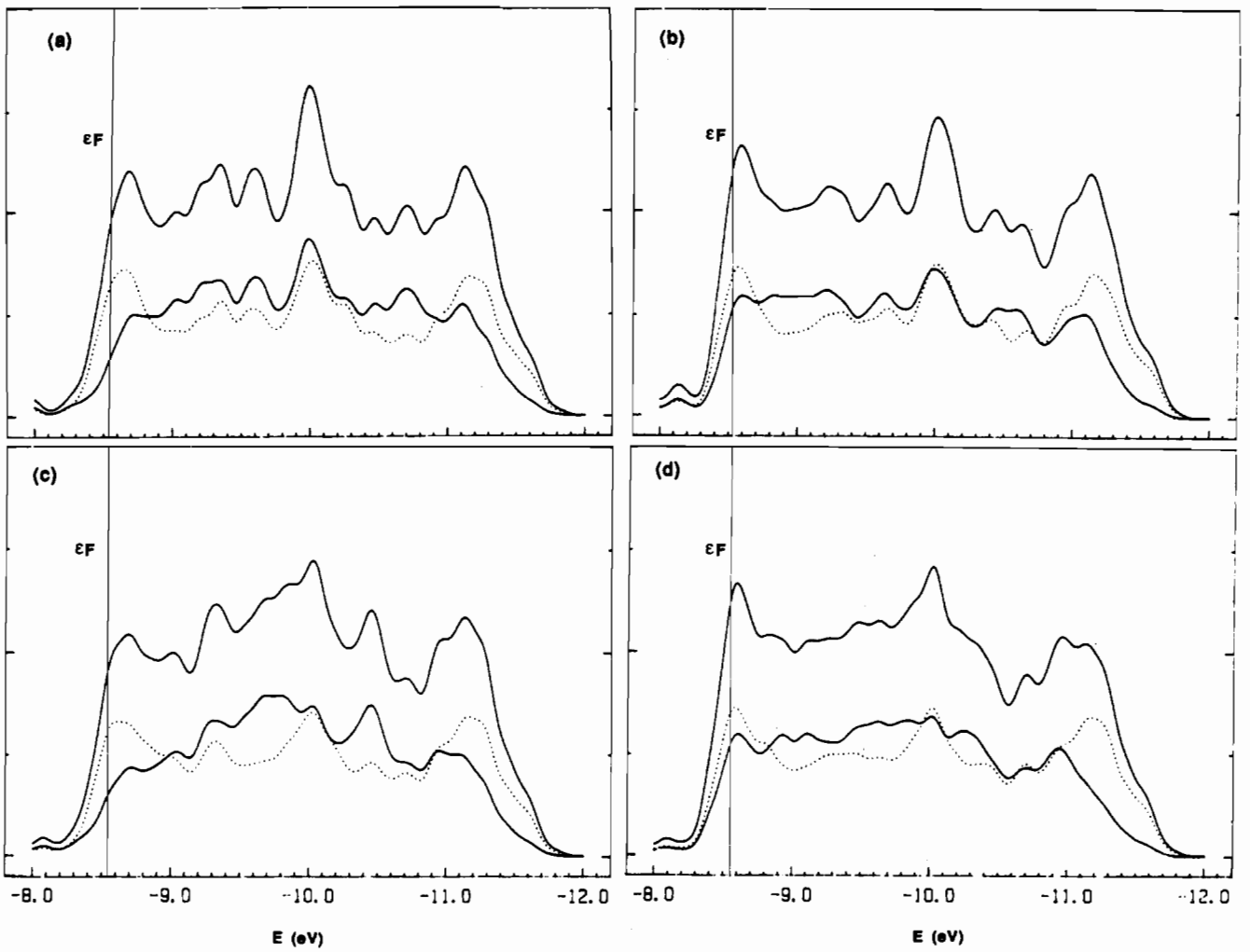

Figure 3. Surface and total electronic densities of states for Ni(110): an unreconstructed surface (a) without oxygen adsorption and (b) with oxygen adsorption; a reconstructed surface (c) without oxygen adsorption and (d) with oxygen adsorption. The Fermi level for nickel is shown. The dotted curve shows the bulk density of states, the solid line close to it the surface density of states, and the third curve the sum of the two.

Pair Potential and Oxygen on a (110) Surface

As we have described above, perhaps the best example of a missing-row reconstruction which is driven by the adsorbate is associated with the adsorption of oxygen atoms on Ni(110),[6] where there is a 2×1 pattern. There is a serious restriction imposed by the tight-binding approach which needs to be circumvented when this problem is studied. The obvious approach is to compute the energy difference between the surface with and without the rows of atoms. However, when the coordination numbers are very different between the two systems to be studied, the method is usually not at all reliable and the results we would obtain would be worthless. Other studies[23,25] which have recognized the limitations of such a model have included an extra classical potential between the atoms of the system in order to overcome this drawback. However, as we will see, calculation of the pair potential between such rows of atoms provides a very useful way to study this problem.

The concept of the pair potential is commonly used to understand the ordering patterns of atoms and molecules adsorbed on metal surfaces and of atoms in solids. For example, oxygen atoms on W(211) (bcc structure) are located in positions where first nearest neighbors are attractive[26] but second nearest neighbors are repulsive along the channels in the surface. Such pair potentials are rather small in magnitude and control the way the adsorbed species are arranged. In principle, they may be calculated by computation of the electronic energy of a judiciously chosen set of surface structural arrangements. We have recently used the idea of a pair potential between atoms within a molecule or solid to delineate regions of chemical stability. For example,[27] although the pair potential which we compute for two cis CO groups in the stable molecule $Cr(CO)_6$ is close to zero, for the species $Fe(CO)_6$ the pair potential is positive and larger than typical values of the metal–CO bond energy. In this case, the results suggest that the $Cr(CO)_6$ molecule is stable with respect to CO loss, but for $Fe(CO)_6$ the repulsion between two CO's is so large that one of them is ejected. In fact, the $Fe(CO)_6$ molecule is not known; the stable mononuclear iron carbonyl is $Fe(CO)_5$ derived from the hypothetical hexacarbonyl by CO loss. We have used this technique to show how the maxima in the "volcano plots" found experimentally for the efficiency of the hydrodesulfurization[28] process coincide with maxima in the pair potential between surface-bound sulfur atoms, the conclusion being that the rate of reaction is set by sulfur atom loss. We may use a similar procedure to study the stability of the complete oxygenated surface relative to that where one row of metal + oxygen is missing. Figure 5 shows the results of the calculation, using the method described in the Appendix.

First consider the plots shown in Figure 5a. The pair potentials are close to zero for bare nickel, indicating that the surface arrangement is a stable one. This is in accord with the observation that these clean surfaces do not reconstruct. However, on adsorption of oxygen, the crossing point of the pair potential has moved so that now for nickel it has become repulsive, indicating

(25) Reindl, S.; Aligia, A. A.; Bennemann, K. H. *Surf. Sci.* **1988**, *206*, 20.
(26) Tringides, M.; Gomer, R. *J. Chem. Phys.* **1986**, *84*, 4049.
(27) Burdett, J. K.; Fässler, T. F. *Inorg. Chem.* **1991**, *30*, 2859. Burdett, J. K.; Fässler, T. F. *Inorg. Chem.* **1991**, *30*, 2859.
(28) Burdett, J. K.; Chung, J. T. *Surf. Sci.* **1990**, *236*, L353.

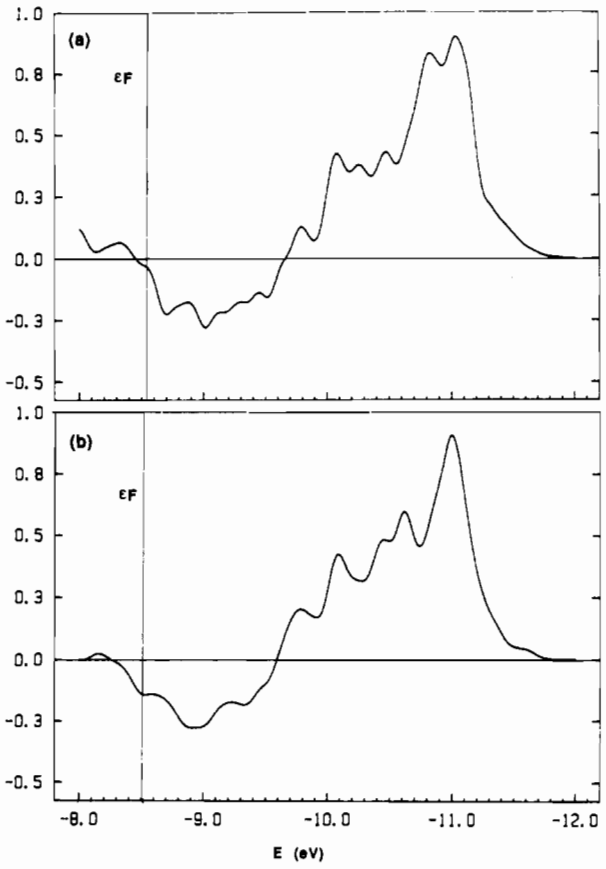

Figure 4. Crystal orbital overlap population (COOP) curves for the Ni–Ni linkage along the short axis of the unreconstructed (110) surface: (a) without and (b) with adsorbed oxygen. The Fermi level for nickel is shown.

instability of adjacent rows of atoms. Schematically the results of this "Gedanken" experiment are shown in Figure 6. One row of metal atoms is ejected on adsorption of oxygen. It is important to realize, however, that in practice metal atoms are not actually vaporized from the surface. The result is nicely in agreement with experiment. Figure 5b shows a similar calculation for a Ni(100) surface. Experimental results are available for copper (a reconstruction of some type does occur) but not for nickel. Later we will present a simple model to show how this variation in pair potential may be understood, which will lead to quite a simple electronic explanation for the adsorbate-induced reconstruction of these metals. It is interesting to ask whether other types of reconstructions might be predicted from the pair potential result. We will show in a separate paper how "defect" type structures can arise too.

It is pertinent to describe how the important features of this pair potential curve vary with the parameters of the calculation. As we show in Figures 3 and 4, the electron counts of interest locate the Fermi level close to the top of the d band of these metals. It is here, using the extended Hückel model, that the wave function, antibonding between many of the metal atoms and with an energy strongly controlled by the values of the interorbital overlap integrals, is most sensitive to changes in geometry and orbital parameters. The calculations reported in Figure 5a used orbital parameters appropriate for nickel. Changes do occur if copper parameters (distances, orbital exponents, and energies) are used in their stead or if the input orbital energy separation of the 3d and 4s orbitals is adjusted (renormalized orbitals). The forms of the pair potentials remain quite similar, but the crossing points are quite parameter sensitive. Figure 5c shows results for Ni(100) using a shorter Ni–O distance. Notice that the shift of the crossing point to the left increases with the strength of the metal–oxygen interaction through this shortening of the metal–oxygen distance. Figure 5d shows results for (110) surfaces using geometries appropriate for nickel and copper. We noted in the Introduction that there did not seem to be an electron-counting rule which controlled the reconstruction, and this may certainly be understood in terms of the parameter sensitivity of the calculations described here.

The behavior of the pair potential curves on oxygen addition has some similarities to the behavior of the COOP curves of Figure 4. There, notice that the contribution to the Ni–Ni overlap population, close to nonbonding at the nickel electron count for the bare surface, becomes repulsive on oxygen coordination. Overall though, as we have pointed out, there seems to be little change in the total bond overlap population itself.

CO on a (110) Surface

The experimental results from studies of the surface structure of Ni(110)[19] in the presence of adsorbed CO show that the surface does not reconstruct in the presence of adsorbate, but there is some debate as to how the CO molecules are adsorbed. There are three possible sites (See Figure 1 for a view of the surface), the on-top sites and the long- and short-bridge sites. CO is an unlikely

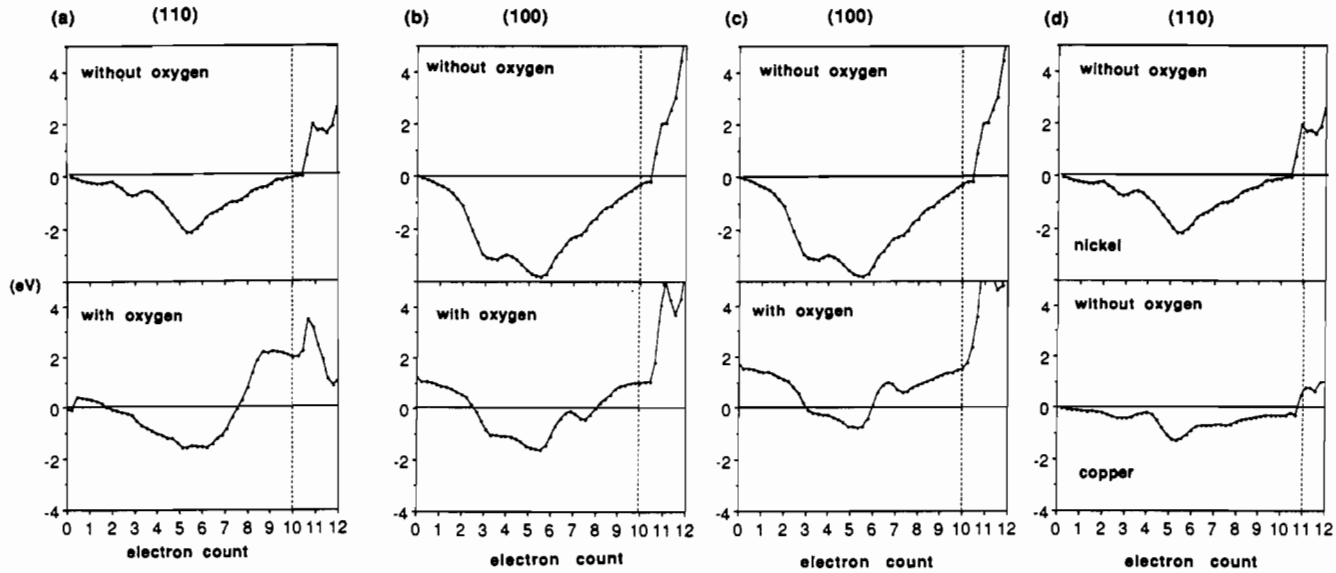

Figure 5. Computed pair potentials between rows of surface nickel atoms as a function of metal electron count: (a) potential for a Ni(110) surface with and without adsorbed oxygen; (b) corresponding results for a nickel (100) surface for a Ni–O distance of 1.93 Å; (c) potential for a Ni(100) surface with and without adsorbed oxygen for a Ni–O distance of 1.77 Å; (d) comparison of the results for (110) surfaces using nickel and copper parameters. In (a)–(c) the nickel electron count is indicated with a dashed line. In (d) the copper electron is similarly labeled.

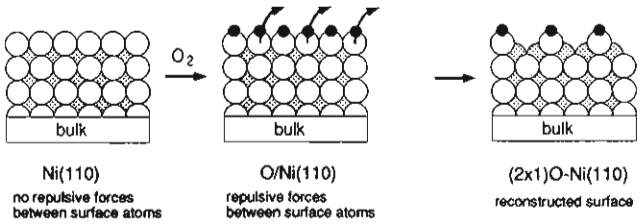

Figure 6. Schematic showing "ejection" of a row of metal atoms when the pair potential becomes repulsive.

occupant of the long bridge because of the metal atom separation here, which leaves the two other possibilities. Presumably because of CO/CO repulsions the adsorbed molecules are arranged in a zigzag fashion along the chain.[20] **2** and **3** show straight and zigzag

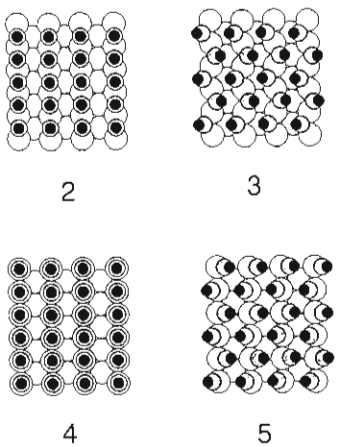

patterns which have been suggested for short-bridge occupation. **4** and **5** show straight and zigzag patterns for top-site occupancy. Figure 7 shows the calculated pair potential plots for the two adsorption patterns of **4** and **5**. Missing-row structures are not possible for **2** and **3**, since the bridging CO would lose one of the metal atoms to which it is connected, although the molecule would presumably move into the on-top site. The behavior of the pair potential plots for CO and O adsorption are very similar, although the details of their shapes are different. The results for CO suggest that the surface should reconstruct in the same way as with adsorbed oxygen, but notice the difference in the location of the crossing point for the two models. The model is highly sensitive to the carbonyl geometry. The striking effect of the zigzag geometry of the CO's is to move the crossing point of the pair potential back toward the right, thus reducing the tendency for missing-row formation for nickel. Our calculations also show that as the metal–CO distance increases, so the crossing point moves to the right. As before, for the case of oxygen on nickel, although the forms of the plots are similar in all cases, the locations of the crossing points are quite geometry sensitive. Although the numerical results show that the surface should reconstruct in the way found for oxygen (there may be an alternative energetically favorable reconstruction of course), the way the CO molecules are adsorbed on the surface strongly affects the location of the crossing point in the pair potential and thus decreases this tendency.

Hydrogen on a (110) Surface

Figure 2 shows some experimental results from studies of the surface structure of Ni(110)[17,18] in the presence of adsorbed hydrogen. The hydrogen atoms are suggested to lie in the 3-fold sites, and the experimental data are sufficiently good to show the very interesting pairing of adjacent pairs of rows of surface atoms, apparently controlled by the hydrogen stoichiometry. The pairing only occurs for the coverage $\theta_H > 1.0$. Such a pairing has structural similarities to the Jahn–Teller and Peierls distortions of molecules and solids. This geometry change is very different from that described for the oxygen case. The LEED results[16-18] show that the distortion consists of a lateral shift of the atoms

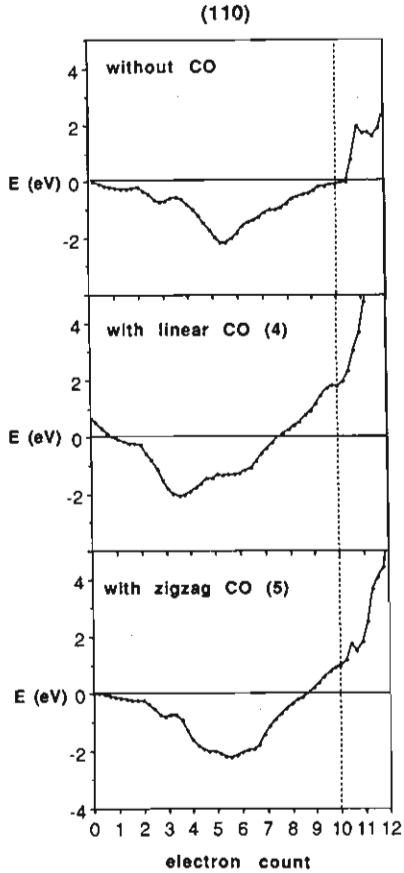

Figure 7. Computed pair potentials (eV) between rows of surface nickel atoms as a function of metal electron count. Shown are the potentials for a Ni(110) surface with and without adsorbed carbon monoxide and the result of tilting the adsorbed molecules (**4** → **5**).

and some vertical buckling of the atoms in the second layer. There is probably some distortion of the third layer too. We will divide our discussion here into two parts, the first associated with the structural changes expected for a single surface layer and the second with the energetics of a metallic slab used to mimic the behavior of the real surface. We will not try to answer the difficult question as to why oxygen and hydrogen behave differently. This may well be determined by the different coordination chemistries of the two atoms, 3-fold versus 2-fold coordination here, a factor which is very difficult for us to probe.

We begin with the electronic description of a single sheet of the (110) surface. The electronic density of states of the sheet is shown in Figure 8a along with its orbital decomposition. The $x^2 - y^2$ and xy bands have the largest width, commensurate with the strong overlap (σ and π, respectively) with their neighbors along the chain direction. Upon reconstruction (Figure 8b), a large portion of each band, particularly the $x^2 - y^2$, is pushed above ϵ_f as a result of the new alternating short–long arrangement of the chains themselves. Figure 9 shows the computed energy difference plot between the distorted and undistorted geometries. Notice that this comprises a broad curve, typical of a significantly different second moment[29] between the two structures, on which is superimposed at high electron counts the characteristic set of oscillations associated with a fourth-moment problem. As we have shown elsewhere, Jahn–Teller and Peierls distortions generally show signatures of this type.[29-31]

Parts a and b of Figure 10 show computed energy difference plots using the Hückel method for the two classic molecular and solid-state examples of structural instabilities of each type, namely the distortion of square cyclobutadiene (to a rectangle) and the

(29) Burdett, J. K.; Lee, S. *J. Am. Chem. Soc.* **1985**, *107*, 3050.
(30) Burdett, J. K. *Struct. Bonding* **1987**, *65*, 30.
(31) Burdett, J. K. *Acc. Chem. Res.* **1988**, *21*, 189.

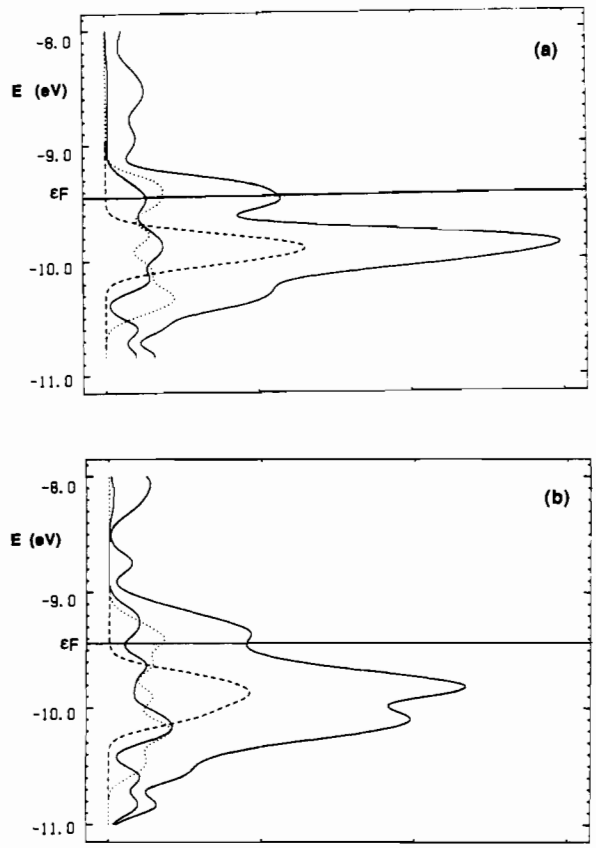

Figure 8. Partial and total electronic densities of states for a single clean sheet of Ni(110). That for an unreconstructed surface without hydrogen adsorption is shown in (a) and that for the reconstructed surface in (b). The dotted curve shows the density of states associated with the xy orbital, the dashed curve that for xz, the solid line close to them for $x^2 - y^2$, and the third curve the total density of states. The short bridges of the surface-atom rows lie along the x direction. The Fermi level indicated is that appropriate for nickel with $\theta_H = 1.0$.

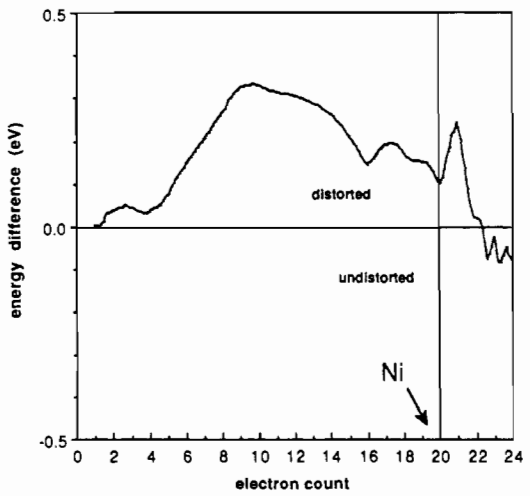

Figure 9. Energy difference curve (for a two-atom cell) between the unpaired and paired structures of Figure 2 for a single surface sheet.

distortion of the simple cubic structure of the group 15 elements (to the α-arsenic or black phosphorus structure). Shown too in Figure 10c is an enlargement of the oscillations between 15 and 21 electrons per two-atom cell for the metal surface layer problem. In all three cases, a structure with equidistant atoms is converted into one where the distances alternate in length. In terms of the behavior of the electronic density of states on distortion, these problems are also similar. A maximum in the density of states at the most favored electron count for distortion is found, which is replaced by a minimum in the distorted structure. A generic picture for the arsenic case is shown in Figure 10d. Figure 11

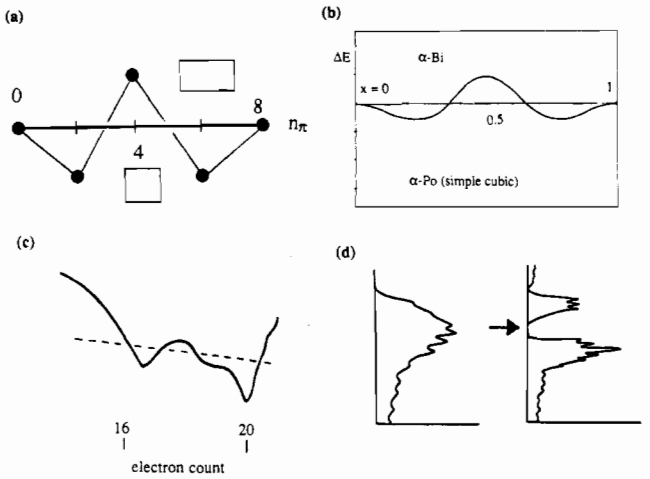

Figure 10. Some computed energy difference plots for Jahn–Teller and Peierls instabilities: (a) distortion of square cyclobutadiene to a rectangle; (b) distortion of the simple cubic structure to that of α-arsenic; (c) enlargement of the oscillations of Figure 9. The dashed line is drawn to guide the eye only. Part d shows an opening of a gap in the electronic density of states on distortion for the α-arsenic case.

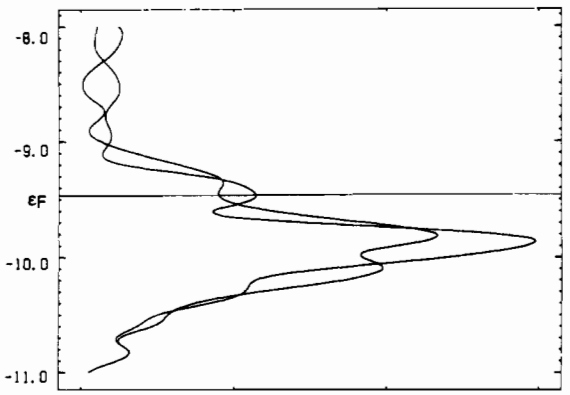

Figure 11. Composite of the two density of states plots of Figure 8, showing a splitting of the density of states on distortion. The Fermi level indicated is that appropriate for nickel with $\theta_H = 1.0$.

shows a composite of the two total density of states plots of Figure 8. The computed distortion for the single sheet thus does indeed appear to be of the Peierls type, although from our calculations the dominant feature of the plot is a second moment, one associated with the fact that the decrease in one set of Ni–Ni distances is not counterbalanced by the increase in the other set. Just as in the molecular case, addition of hydrogen might be expected to strongly influence the distortion. Recall that addition of hydrogen to cyclobutadiene to give cyclobutane suppresses the tendency for bond alternation. It becomes useful to regard the addition of hydrogen to the surface as leading to surface oxidation, thus changing the effective electron count for a given metal and changing the energetics accordingly.

As expected, the real surface picture is very complex and depends upon the geometric details of the distortion and the site preference of the adsorbed ligands. Given the approximate nature of the structure determination for this reconstruction, we selected two distortions for study. Two computed energy difference curves are shown in each panel of Figure 12 for the relative stability of the unreconstructed an reconstructed nickel slab. The calculation used a double-sided slab containing five "bulk" atoms, and the distortion took place on both sides. They represent comparison with the experimentally observed reconstruction (curve a) and a top-layer row-pairing model we call a "circular distortion" (curve b). The observed distortion consists of pairing of the top rows accompanied by a buckling of the second layer while the circular distortion changes the spacing of the surface layer while keeping the interatomic distances to the second layer unchanged, as if being moved along the circumference of a circle. In our view, this model

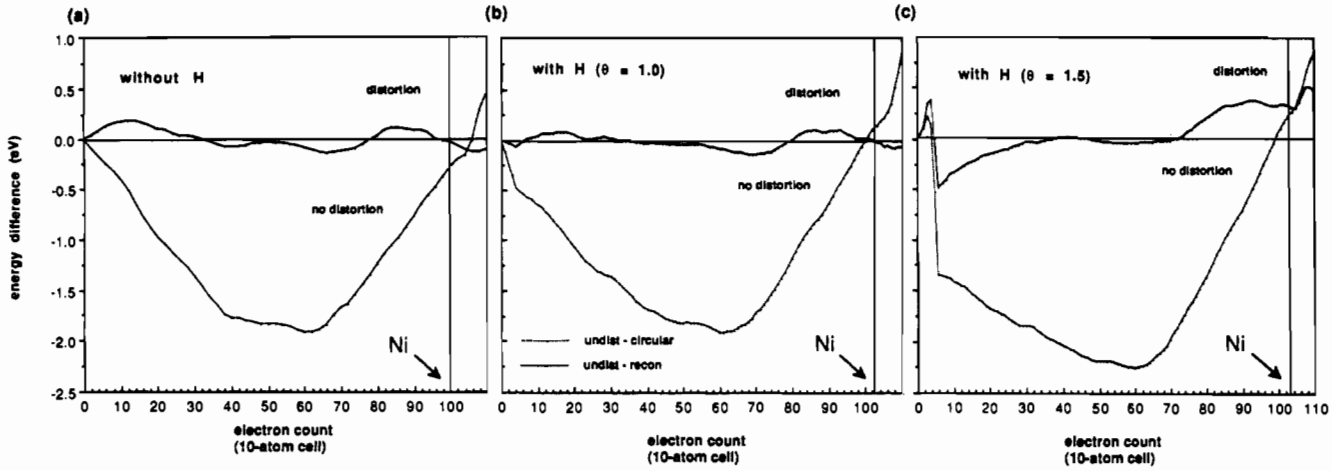

Figure 12. Computed energy difference curves (eV) for the pairing distortion of Figure 2 as a function of electron count: (a) bare surface; (b) surface with two adsorbed hydrogen atoms per surface cell (θ = 1); (c) surface with three adsorbed hydrogen atoms per unit cell (θ = 1.5). Two curves are shown for each case. The curve with the larger amplitude represents the "circular" distortion where the distances between the surface and second-layer atoms are kept fixed and the surface atoms paired up by moving them along an arc of a circle. The other curve shows the results of a set of calculations using the complete geometrical reconstruction reported in refs 16–18.

mimics the one-layer calculation "in a field of" the rest of the bulk, thus isolating the effect of changes to the first layer while accounting for the rest of the bulk. Parts b and c of Figure 12 show energy difference curves for the undistorted and the distorted geometries with differing amounts of adsorbed hydrogen bound to the surface in 3-fold sites. Though widely differing stabilities occur while the bands of all three sets of curves are being filled with electrons, at the particular electron counts of interest, there is a clear progression favoring reconstruction with addition of hydrogen. Interestingly, both models of the surface reconstruction show the same energetic behavior on hydrogen coordination. As indicated by the vertical lines, the curves just barely favor the undistorted surface for a bare nickel slab, nearly reproduce the observed crossing point for two hydrogen atoms per cell, and clearly favor a reconstruction for a hydrogen coverage of θ_H = 1.5 or a structure with three hydrogen atoms per unit cell. The trend on addition of hydrogen found experimentally is correctly reproduced, although we should bear in mind the inability of current methods to determine the exact location of the adsorbed atoms. The curves strongly suggest that though significant second-row buckling and third-row pairing may be observed, the driving force for the Ni(110) reconstruction may be associated with the chemistry of the surface atoms. Interestingly, the curves for the circular distortion show a typical second-moment shape that has striking similarities to the computed pair potential for the oxygen case (Figure 5) and the molecular analogue presented below.

A Molecular Model

In the Introduction we noted that surface reconstructions of main-group systems were, in principle, easier to understand than those associated with transition metals. This came about simply as a result of the ability to use two-center–two-electron bonding models in the main-group regime but not for the transition metal case. In this section we will describe a main-group problem which has electronic and structural features very similar to those we have described here. In addition, it is a molecular system. It is one where simple Lewis ideas provide a ready understanding of the electronic situation and thus will allow us to build a bridge to the complex surface results described earlier.

The general result that oxidation of the surface atoms by coordination of oxygen or hydrogen induces a geometrical rearrangement reminds us of very similar behavior in the molecular situations shown in **6**. Certainly, the species in the series N_2,

B_2 C_2 N_2 O_2 F_2 (Ne_2)

B_2H_2 C_2H_2 N_2H_2 O_2H_2 $(F_2H_2$ $Ne_2H_2)$

6

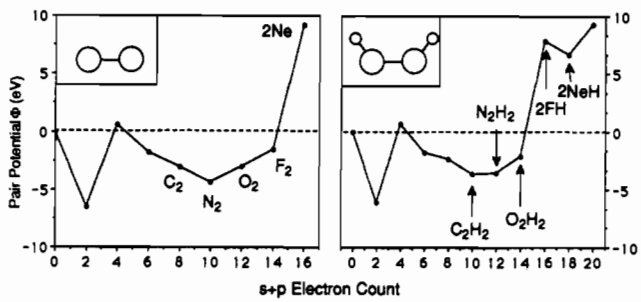

Figure 13. Pair potential (eV) calculated between the A atoms for (a, left) the second-row A_2 series and (b, right) the second-row A_2H_2 series. In this case the pair potential is simply the A–A bond energy.

O_2, F_2 are stable as diatomic molecules (Figure 13a), but the end member of the series N_2H_2, O_2H_2, F_2H_2 is unstable with respect to fission into two HF units. Figure 13b shows a calculated energy difference curve for the process $F_2H_2 \rightarrow 2HF$. Although we hasten to add that numerically the values obtained from such a one-electron calculation are not to be trusted, the shapes of the plots are completely in accord with the observed chemistry. F_2 is stable with respect to bond breaking, but F_2H_2 is not. These curves are remarkably similar to those of Figure 5 for the metal surface reconstruction. Thus, the nickel surface without oxygen (analogous to F_2) is stable to atom loss, but the surface with oxygen (analogous to F_2H_2) is not. Of course, we reiterate that this atom loss process is a Gedanken experiment—the metal atoms close to the surface rearrange so that no metal atoms are actually lost into vacuum.

A similar model may be used for the pairing distortion induced by hydrogen adsorption. Here, the corresponding molecular situations are shown in **7**. Unlike the molecules in **6**, several of

Al_4 Si_4 P_4 S_4 (Cl_4)

Al_4H_4 Si_4H_4 P_4H_4 $(S_4H_4$ $Cl_4H_4)$

7

these do not exist. However, from the *Lewis* point of view, there is nothing wrong with the stability of species such as Si_4 or open chain P_4. The S_4^{2-} species, and indeed longer S_n^{2-} chains, do exist. Thus, whereas the S_4 chain is stable to bond fission, the H_4S_4 chain (with two extra electrons) is unstable with respect to a "pairing" distortion to give two H_2S_2 molecules. Again, the energy difference curves for the distortion (Figure 14), with and without "adsorbed" hydrogen, are similar to those of Figure 12. A similar type of bond-breaking process occurs in many areas of chemistry; for example, on moving from tetrahedral P_4 (six P–P bonds) to P_4(cyclohexyl)$_4$ (four P–P bonds), two linkages are broken. Of course, both sets of molecular examples (F_2/F_2H_2 and S_4/H_4S_4)

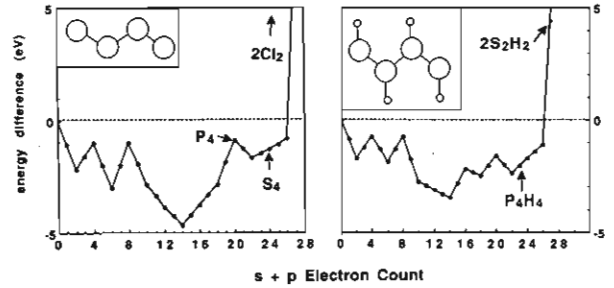

Figure 14. Pair potential (eV) calculated between the central pair of A atoms for (a, left) the third-row A_4 series and (b, right) the third-row A_4H_4 series. In this case the pair potential is simply the central A–A bond energy.

are understandable using very traditional ideas of chemical bonding. In the surface transition-metal case no such simple Lewis picture is appropriate.

Conclusion

Tight-binding calculations within the extended Hückel formalism have enabled us to examine the driving forces of several adsorbate-induced reconstructions of the Ni(110) surface. Adsorbed rows of oxygen atoms on nickel have a calculated repulsive pair potential, indicating the instability of adjacent rows of atoms and thus driving the "missing-row" reconstruction for this system. A similar reconstruction is suggested for adsorbed carbon monoxide though the actual crossing point of the pair potential is extremely sensitive to the geometry of the CO molecules. In addition, the complex row-pairing–row-buckling reconstruction mechanism for H on Ni(110) is traced to the dominant electronic effects at the top layer. Finally, we present molecular analogues for these systems in order to draw attention to the striking similarities in their calculated energy difference curves.

The rather interesting results for the single layer of the Ni(110) system lead us to ask whether it may be possible to study experimentally the geometries of single layers of metal atoms. This would clearly require a support of some type with rather special properties. In order to preserve a single layer, the tendency for the metal atoms to cluster needs to be overcome by provision of moderate support–metal atom interactions. Of course, if these are strong, the geometry is determined by these effects rather than by the desires of the metal sheet. We are encouraged though by the recent results of Gomer and co-workers,[32] who have prepared a single layer of copper atop a layer of CO, itself supported on a tungsten surface.

Acknowledgment. Thomas Fässler thanks the Deutsche Forschungsgemeinschaft for a fellowship, and Paul Czech, The Midstates Pew Cluster for a Teacher-Scholar Award. The research was supported by the National Science Foundation (Grant DMR8819860) and by The University of Chicago.

Appendix

The calculations were carried out with the extended Hückel implementation of tight-binding theory.[33] The atomic parameters used are given in Table I. For the calculations on the unreconstructed and reconstructed Ni(110) surfaces, slabs composed of eight and nine layers of metal atoms, respectively, were used. Whereas, for the determination of DOS and COOP plots, convergence of the results is obtained with a smaller number of layers, the pair potential plots require this number for convergence. In order to obtain comparable results in all cases (unreconstructed, reconstructed, with and without oxygen or CO, respectively) a rectangular set of 16 k points was used, even when higher symmetry was present. The metal–metal distances in each case were taken as their bulk values. For the substrates, the following distances were used. O/Ni(110) system: Ni(surface)–O = 1.77 Å, O in long-bridge position; Ni(surface)–C = 1.80 Å, C–O = 1.15 Å (CO on top and in short-bridge position). O/Ni(100) system: Ni(surface)–O = 1.93 and 1.77 Å, respectively, O in 4-fold hollow sites. H/Ni(110) system: Ni(surface)–H = 1.60 Å, H in 3-fold sites.

To calculate the pair potential $\Phi(x)$ between two surface rows, we used the technique described previously.[27] Essentially, the pair potential is the energy difference between the bond energy appropriate for two units, X and Y, attached to the surface concurrently and that expected if the two were attached separately. X and Y might be surface-adsorbed molecules if we were interested in the pair potential between them; here, they are rows of "surface" atoms. Its evaluation requires three calculations for each electron count: the bond energy of X with respect to fragment A

$$\begin{aligned} BE_0 &= E(AX) - E(A + X) \\ &= E(AX) - E(A) - E(X) \end{aligned} \quad (1)$$

the bond energy of X with respect to fragment AY

$$\begin{aligned} BE_1 &= E(AYX) - E(AY + X) \\ &= E(AYX) - E(AY) - E(X) \end{aligned} \quad (2)$$

the pair potential, Φ, between X and Y

$$\begin{aligned} \Phi &= BE_1 - BE_0 \\ &= [E(AYX) - E(AY) - E(X)] - [E(AX) - E(A) - E(X)] \\ &= [E(AYX) + E(A)] - [E(AX) + E(AY)] \end{aligned} \quad (3)$$

For X = Y, as in the present case

$$\Phi = [E(AX_2) + E(A)] - 2E(AX) \quad (4)$$

This is shown in **8** for the case of the (110) surface. To keep the stoichiometry constant within the calculation of Φ for a given surface, the row or pair of rows of atoms were included in the calculation but with no overlap with the bulk.

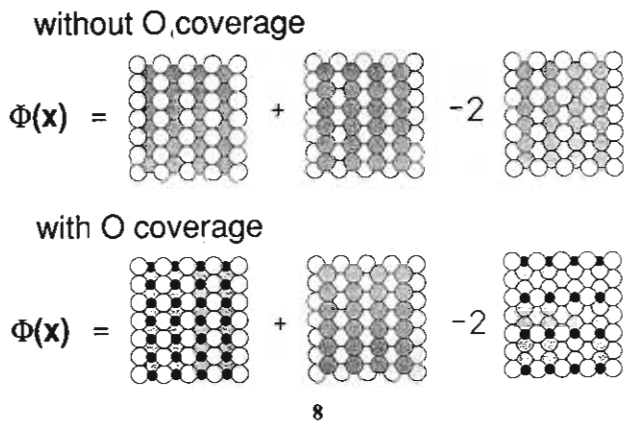

8

The geometry for the hydrogen-induced reconstruction involved two distortions. First, there is a lateral shift of the evenly spaced top-layer rows (3.52 Å apart) to the row-paired geometry (2.92 Å apart). Second, a buckling of the second-row atoms, essentially an alternating displacement of ±0.25 Å along the vertical or z axis occurs. The so-called "circular" distortion retains the row-pairing aspect of the observed reconstruction but does not change the (close-packed) bond distance of 2.50 Å to the second layer.

Registry No. CO, 630-08-0; H_2, 1333-74-0; O_2, 7782-44-7; Ni, 7440-02-0.

(32) Liu, C.; Shamir, N.; Gomer, R. *Surf. Sci.* **1990**, *261*, 26. Liu, C.; Shamir, N.; Gomer, R. *J. Chem. Phys.* **1989**, *90*, 5135.
(33) Hoffmann, R.; Lipscomb, W. N. *J. Chem. Phys.* **1962**, *36*, 2179; **1962**, *37*, 2872. Whangbo, M.-H.; Hoffmann, R.; Woodward, R. B. *Proc. R. Soc. London* **1979**, *A366*, 23.